Peptide Design

DOI: 10.1002/anie.200800677

Cyclic Peptides Bearing a Side-Chain Tail: A Tool to Model the Structure and Reactivity of Protein Zinc Sites**

Olivier Sénèque, Emilie Bourlès, Vincent Lebrun, Estelle Bonnet, Pascal Dumy, and Jean-Marc Latour**

A recent bioinformatics study has evaluated to about 1000 (or ca. 3% of the total protein number) the number of human proteins possessing a tetracysteinate zinc site.[1] These sites were initially presumed to have a structural role because they were associated to zinc finger proteins,[2] where they fold the protein chain in a conformation suitable for its binding to DNA. They were later found in several proteins and enzymes involved in demethylation processes, such as the DNA repair protein Ada[3] and various transferases.[4] More recently, such sites were discovered in the heat shock protein Hsp33[5] and the disulfide reductase Trx2,[6] where their interaction with reactive oxygen species (ROS) contributes to the oxidative-stress response. This is of special interest as tetracysteinate zinc sites, especially in zinc finger proteins, have been considered to be likely targets of ROS. Free cysteines are commonly involved in peroxide sensing and response,[7] and their reactivity has been thoroughly studied over the past twenty years. A reasonable reactivity picture has emerged that points to the importance of hydrogen bonding in increasing the nucleophilic character of the cysteine sulfur atom. No such rationale is available for metal-bound cysteinates.

To obtain a better understanding of the reactivity of tetracysteinate zinc sites with ROS, we are developing a biomimetic approach based on de novo peptide synthesis. This approach is particularly suited to mimicking these sites and the potentially important hydrogen-bonding interactions, which is not possible with metallo-organic complexes in organic solvents. The validity of this approach has been demonstrated by Berg and Shi in their modeling studies of zinc finger proteins with a mixture of cysteinate and histidine ligands,[8] and was further highlighted more recently by Gibney et al.[9] Both groups used linear 16- to 26-mer peptides incorporating two CX_nC ($n = 2$–4) zinc-binding motifs. Regan and Clarke[10] relied on self-assembling peptides to constitute a four-helix bundle orienting the cysteinates in the proper way to bind zinc. Nevertheless, this approach is generally weakened by the difficulty of obtaining detailed structural characterization of metallopeptides. In addition, these two designs cannot reproduce the tetracysteinate arrangements that belong to β hairpins, such as that of Hsp33.[5]

This prompted us to develop a totally new design based on introducing one CX_nC motif into a cyclic peptide and another one into a linear chain connected to the cycle through a glutamate or lysine residue. Herein, we show that these peptides with limited size and flexibility, allow the almost perfect reproduction of both the structure and the reactivity of the tetracysteinate zinc site of the protein Hsp33.

Figure 1 illustrates the tetracysteinate zinc site of Hsp33, which consists of a CXXC motif ($C_{263}KWC_{266}$) located in a β-hairpin loop and a CXC motif ($C_{231}DC_{233}$). To reproduce the topology of this site, we designed a cyclic peptide to mimic the β-hairpin loop[11] and a linear tail was grafted on one of the side chains of the loop to introduce the CXC motif. The D-Pro-L-Pro dipeptide template was used to preorganize the ten residues constituting the β-hairpin loop.[11] The linear tail

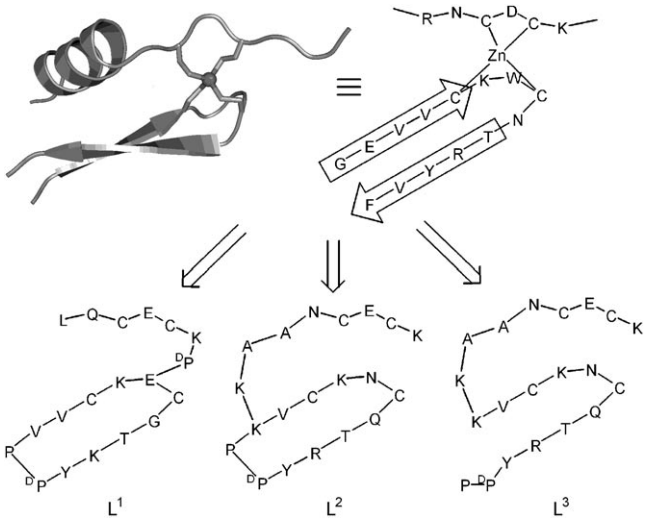

Figure 1. Design of model peptides. Part of the crystallographic structure of *Thermotoga maritima* Hsp33[5] showing the $Zn(Cys)_4$ site (top left), its schematic representation (top right), and the model peptides L^1, L^2, and L^3 (bottom). Some of the amino acids were changed in the models to prevent overlapping in the NMR spectra.

[*] Dr. O. Sénèque, Dr. E. Bourlès, E. Bonnet
Laboratoire de Chimie et Biologie des Métaux, CNRS UMR 5249
17 rue des Martyrs, 38054 Grenoble (France)
Fax: (+33) 4-3878-3462
E-mail: olivier.seneque@cea.fr

V. Lebrun, Dr. J.-M. Latour
CEA, iRTSV, LCBM
17 rue des Martyrs, 38054 Grenoble (France)
Fax: (+33) 4-3878-3462
E-mail: jean-marc.latour@cea.fr

Prof. Dr. P. Dumy
Département de Chimie Moléculaire, UMR CNRS-UJF 5250
Université Joseph Fourier, Grenoble (France)

[**] The authors thank Mrs. C. Lebrun for access to the ESI mass spectrometer and the Agence Nationale de la Recherche (ANR-06-JCJC-0018) for financial support.

Supporting information for this article is available on the WWW under http://dx.doi.org/10.1002/anie.200800677.

was grafted on a Glu residue of the cycle through its N end (peptide L^1) or on a Lys residue through its C end (peptide L^2). The linear precursor of L^1 was assembled on Sieber amide resin by using 9-fluorenylmethoxycarbonyl (Fmoc) chemistry. Fmoc-Glu-OAll was used to create the branching point between the two parts of the peptide (Scheme 1). After selective removal of the allyl group with Pd^0, cleavage from the resin with 1% trifluoroacetic acid (TFA) in CH_2Cl_2 yielded a linear peptide amidated at the C-terminal leucine and still bearing the side-chain protecting groups. Cyclization between the only two unprotected functions (main-chain Glu-COOH and Cys-NH_2) in CH_2Cl_2 followed by removal of the side-chain protecting groups by TFA/triisopropylsilane (TIS)/H_2O/dithiothreitol (DTT) and purification by HPLC yielded L^1.

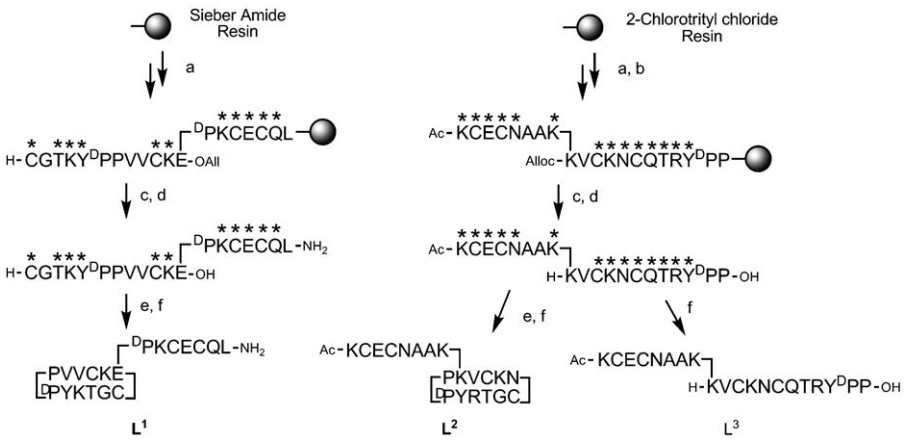

Scheme 1. Synthesis of peptides L^i ($i = 1$–3). a) Fmoc SPPS; b) DMF/pyridine/Ac_2O (7:2:1); c) [Pd-(PPh_3)$_4$], $PhSiH_3$, CH_2Cl_2; d) CH_2Cl_2/TFA (99:1); e) 0.25 mM, PyBOP, DIEA, CH_2Cl_2; f) TFA/TIS/H_2O/DTT. * denotes side-chain protecting groups. SPPS = solid-phase peptide synthesis, DMF = dimethylformamide, PyBOP = (benzotriazol-1-yloxy)tripyrrolidinophosphonium hexafluorophosphate, DIEA = *N*,*N*-diisopropylethylamine. For the one-letter code of amino acids see for example http://www.chem.qmul.ac.uk/iupac/AminoAcid/AA1n2.html.

The peptide L^2 was synthesized in a similar way on 2-chlorotrityl chloride resin by using allyloxycarbonyl-Lys-(Fmoc)-OH to introduce the branching point. To assess the value of the design described above, L^3, the linear analogue of L^2, was synthesized by suppressing the cyclization step. All peptides were identified by ESI mass spectrometry (ESI-MS) and ^{1}H NMR spectroscopy.

Metal binding was investigated by UV/Vis spectroscopy, CD, and fluorescence titrimetry at pH 7.0. Titrations with Co^{2+} showed the formation of a unique 1:1 complex Co·L^i for each of the three peptides. The ligand-to-metal charge-transfer (LMCT) and d–d transitions of these complexes are consistent with a Co^{2+} ion coordinated by four cysteinates in a tetrahedral geometry (Table 1).[12] The d–d transition patterns of the three Co·L^i complexes differ quite significantly but the spectra of Co·L^2 and Co·Hsp33[13] are strikingly similar (Figure S1 in the Supporting Information).

With Zn^{2+}, the three peptides exhibit distinct behaviors. L^2 forms only a 1:1 complex (Zn·L^2), whereas L^3 also forms a complex of undefined stoichiometry in excess of zinc, and L^1 forms a 1:2 Zn·$(L^1)_3$ complex, detected during CD titration in conditions of excess peptide. The LMCT band of the Zn·L^i complexes around 210 nm indicates that the metal is coordinated by the four thiolates.[14] The apparent binding constants are $10^{9.9(2)}$ and $10^{8.6(2)}$ at pH 7.0 for Co·L^2 and Co·L^3, respectively, and are $10^{16.3(2)}$ and $10^{15.2(2)}$ for Zn·L^2 and Zn·L^3, respectively, at pH 7.5. Thus, the complexes formed by the cyclic peptide L^2 are more stable than those of its linear analogue L^3 by approximately one order of magnitude. The value measured for Zn·L^2 is very similar to that reported for Zn·Hsp33 ($10^{16.6}$) at pH 7.5.[15]

Table 1: UV/Vis characterization of Co^{2+} and Zn^{2+} complexes of peptides L^i at pH 7.0.

Complex	λ [nm] ($\Delta\varepsilon$ [$M^{-1}cm^{-1}$])
Co·L^1	302 (6460), 360 (3980), 645 (630), 685 (835), 726 (930)
Co·L^2	300 (4270), 347 (3200), 635 (369), 686 (769), 722 (697)
Co·L^3	310 (4080), 356 (2860), 617 (408), 680 (570), 741 (407)
Zn·L^1	213 (19600)
Zn·L^2	204 (23700)
Zn·L^3	211 (20600)

The structures of the zinc complexes were investigated by ^{1}H NMR spectroscopy. Zn·L^1 and Zn·L^2 display well-resolved spectra, whereas Zn·L^3 shows broad peaks characteristic of conformational motion (Figure 2). Thus, only the cyclic-peptide-based models Zn·L^1 and Zn·L^2 are suitable for detailed structure determination. Their NH resonances are spread over the 7–9.5 ppm range, most of the $^3J_{NH,H\alpha}$ values are out of the 6–8 Hz range, and a large number of NOE cross-peaks are observed between the cycle and the tail (see the Supporting Information). This clearly indicates that Zn·L^1 and Zn·L^2 adopt a well-defined conformation. The numerous cross-strand NOEs show that the cycle folds in a regular β hairpin.[16] The NOE pattern of the four cysteine

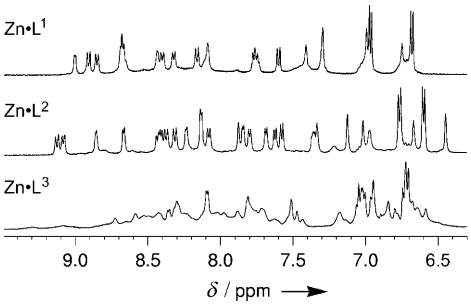

Figure 2. NH and aromatic region of the ^{1}H NMR spectra (500 MHz, 298 K, H_2O/D_2O 9:1, pH 6.2) of peptide complexes Zn·L^i prepared by adding 1.0 equiv of Zn^{2+} to the peptide L^i.

residues and the $^3J_{H\alpha,H\beta}$ values show that the positions of the cysteine side chains are well defined.[17] The structure was calculated by using the program X-PLOR 3.851[18] with 247 H–H distance constraints (81 intraresidue, 78 sequential, and 88 medium range) extracted from the NOESY spectra (200 ms) and 12 ϕ and 3 χ_1 dihedral constraints for Zn·L^1, and with 255 H–H distance constraints (91 intraresidue, 66 sequential, and 98 medium range) and 12 ϕ and 4 χ_1 dihedral constraints for Zn·L^2.

The superposition of the lowest-energy structures with the zinc site of *Thermotoga maritima* Hsp33 are depicted in Figure 3. Both model peptides perfectly reproduce the hairpin loop (the backbone root-mean-square deviation is 0.57

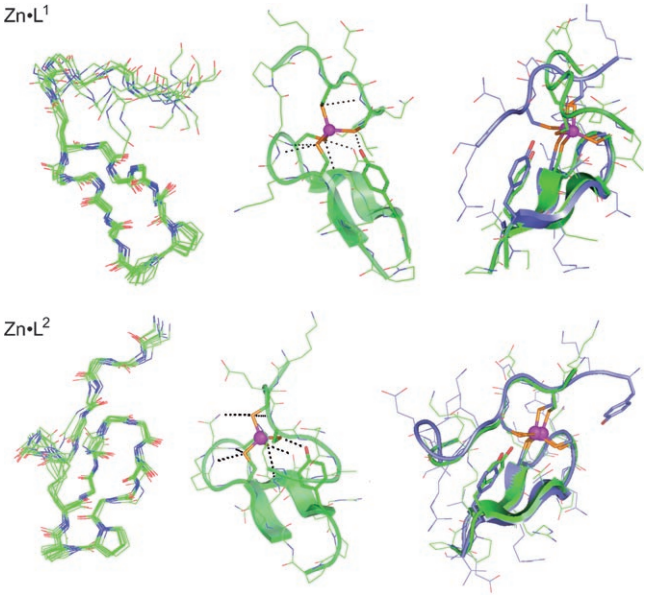

Figure 3. Structures of Zn·L^1 and Zn·L^2 deduced from NMR solution studies. Left: superposition of the ten lowest-energy NMR structures calculated by using X-PLOR. Middle: lowest-energy structure showing the hydrogen-bond network (black). Right: superposition of the lowest-energy structure of Zn·L^i (green) with the zinc site of *T. maritima* Hsp33 (pdb 1VQ0, blue).

and 0.40 Å for Zn·L^1 and Zn·L^2, respectively). The linear tail of Zn·L^1 is slightly tilted from the corresponding sequence in Zn·Hsp33, whereas a perfect match is noted for Zn·L^2 with exactly the same relative orientation for the side chains of the four cysteines. All of the seven hydrogen bonds involving the cysteine sulfur atoms in the X-ray structure of Hsp33 are reproduced in the model compound Zn·L^2 whereas Zn·L^1 lacks one.

In a preliminary reactivity study with ROS, we investigated the oxidation of the three Zn·L^i complexes with H_2O_2. The reaction of Zn·L^i with excess H_2O_2 was followed by ESI mass spectrometry, UV/Vis and fluorescence spectroscopy. Zn·L^i, L$^i_{SS}$, and L$^i_{SS}$ (the peptides presenting one and two disulfides, respectively) were observed by ESI-MS, the latter being the only species at the end of the reaction. Tyrosine fluorescence was recorded as a function of time (Figure 4). The decrease of the fluorescence correlates with the decrease of the LMCT band at about 210 nm monitored by UV/Vis

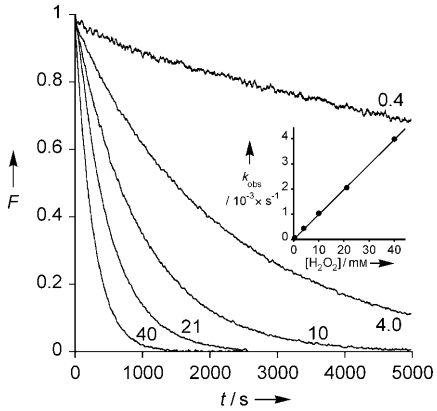

Figure 4. Normalized tyrosine fluorescence changes (λ_{ex} = 280 nm, λ_{em} = 307 nm) observed during reaction of Zn·L^2 (20 μM) with excess H_2O_2 at 298 K and pH 7.0. The numbers denote the H_2O_2 concentrations in mM. Inset: the k_{obs} obtained by fitting each kinetic trace with a single exponential as a function of H_2O_2 concentration.

spectroscopy. Fluorescence kinetic measurements allowed us to monitor the destruction of the Zn(Cys)$_4$ center and the formation of disulfides, which are efficient quenchers of tyrosine fluorescence.[19]

The kinetic traces were perfectly fitted with a single exponential. The apparent pseudo-first-order constant k_{obs} is proportional to the concentration of H_2O_2. Therefore, the oxidation follows a second-order kinetic law $r = k[Zn{\cdot}L^i][H_2O_2]$, which shows that the rate-determining step corresponds to the bimolecular reaction of Zn·L^i with H_2O_2, with a highly ordered transition state as shown by the large negative value of $\Delta S^{\neq}$ derived from Eyring plots (Table 2). Interestingly, the kinetic constants at 303 and 316 K for the best

Table 2: Kinetic parameters for the oxidation of Zn·L^i by H_2O_2.

	Zn·L^1	Zn·L^2	Zn·L^3	Zn·Hsp33[a]
k_{303K} [$M^{-1}s^{-1}$]	0.20 (1)	0.13 (1)	0.57 (2)	0.12 (1)
k_{316K} [$M^{-1}s^{-1}$]	0.45 (2)	0.28 (1)	1.2 (1)	0.31 (3)
$\Delta H^{\neq}$ [kJ mol^{-1}]	47.8 (5)	43.1 (5)	45.1 (5)	–
$\Delta S^{\neq}$ [J mol^{-1} K^{-1}]	−101 (2)	−120 (2)	−101 (2)	–

[a] Kinetic constants were obtained from reference [20] by converting the half-life reaction time of Zn·Hsp33 with 2 mM H_2O_2 using the formula $k = (\ln 2/t_{1/2})/[H_2O_2]$.

structural model Zn·L^2 are in excellent agreement with those deduced from the data reported for Zn·Hsp33.[20] Moreover, it seems that the oxidation kinetics parallel the structural ordering of the zinc site. With one missing hydrogen bond, Zn·L^1 is oxidized more rapidly than Zn·L^2, and consistently the fastest oxidation is observed for Zn·L^3, which has no defined conformation and thus no defined hydrogen-bond network.

In summary, we have devised a new design based on branched cyclic peptides to mimic the tetracysteinate zinc sites belonging to a β hairpin, such as the Zn(Cys)$_4$ site of Hsp33. This is achieved with short peptides (about 20 amino acids) that are easy to synthesize. Moreover, their limited size allows rapid NMR structural characterization, which can

scarcely be achieved with linear peptides or multihelix bundles. The differences between L^2 and L^3 highlight the interest in this design over the use of linear peptides for the modeling of structural properties and reactivity. The comparison between L^1 and L^2 shows that small changes in the structure and in the H-bonding pattern of these complexes can influence their reactivity. The oxidation of these $Zn(Cys)_4$ sites in conditions of severe H_2O_2 stress (100 μM–5 mM) is very slow with half-life reaction times of several minutes, thus suggesting that H_2O_2 might not be the ROS actually responsible for the oxidation in vivo. We are further exploring the reactivity of these promising models towards H_2O_2 and other ROS.

Received: February 11, 2008
Revised: June 16, 2008
Published online: July 24, 2008

Keywords: bioinorganic chemistry · cysteines · NMR spectroscopy · peptides · zinc

[1] C. Andreini, L. Banci, I. Bertini, A. Rosato, *J. Proteome Res.* **2006**, *5*, 196.
[2] J. M. Berg, *Curr. Opin. Struct. Biol.* **1993**, *3*, 11.
[3] H. Takinowaki, Y. Matsuda, T. Yoshida, Y. Kobayashi, T. Ohkubo, *Protein Sci.* **2006**, *15*, 487.
[4] J. Penner-Hahn, *Curr. Opin. Chem. Biol.* **2007**, *11*, 166.
[5] I. Janda, Y. Devedjiev, U. Derewenda, Z. Dauter, J. Bielnicki, D. R. Cooper, P. C. F. Graf, A. Joachimiak, U. Jakob, Z. S. Derewenda, *Structure* **2004**, *12*, 1901.
[6] J. F. Collet, J. C. D'Souza, U. Jakob, J. C. A. Bardwell, *J. Biol. Chem.* **2003**, *278*, 45325.
[7] L. B. Poole, *Arch. Biochem. Biophys.* **2005**, *433*, 240.
[8] Y. G. Shi, J. M. Berg, *Chem. Biol.* **1995**, *2*, 83.
[9] A. K. Petros, A. R. Reddi, M. L. Kennedy, A. G. Hyslop, B. R. Gibney, *Inorg. Chem.* **2006**, *45*, 9941.
[10] L. Regan, N. D. Clarke, *Biochemistry* **1990**, *29*, 10878.
[11] M. Favre, K. Moehle, L. Y. Jiang, B. Pfeiffer, J. A. Robinson, *J. Am. Chem. Soc.* **1999**, *121*, 2679.
[12] A. B. P. Lever, *Inorganic Electronic Spectroscopy*, Elsevier, Amsterdam, **1984**.
[13] U. Jakob, M. Eser, J. C. A. Bardwell, *J. Biol. Chem.* **2000**, *275*, 38302.
[14] M. Vasak, J. H. R. Kagi, H. A. O. Hill, *Biochemistry* **1981**, *20*, 2852.
[15] Jakob et al. measured a binding constant $K_{ZnHps33}$ of $10^{17.4}$ for ZnHsp33 at pH 7.5 by competition experiments with *N*,*N*,*N*′,*N*′-tetrakis(2-pyridylmethyl)ethylenediamine (tpen).[13] The binding constant they used for the [Zn(tpen)] complex was the absolute binding constant ($\beta_{11} = 10^{16}$). The apparent binding constant for [Zn(tpen)] can be calculated by taking into account the protonation constants of tpen. The actual value is $10^{15.2}$ at pH 7.5. Thus, $K_{ZnHps33}$ is $10^{16.6}$ at pH 7.5.
[16] K. Wüthrich, *NMR of Proteins and Nucleic Acids*, Wiley, New York, **1986**.
[17] G. Wagner, W. Braun, T. F. Havel, T. Schaumann, N. Go, K. Wüthrich, *J. Mol. Biol.* **1987**, *196*, 611.
[18] A. Brünger, *A System for X-ray Crystallography and NMR*. X-PLOR, version 3.1, Yale University Press, New Haven, CT, **1992**.
[19] H. Szmacinski, W. Wiczk, M. N. Fishman, P. S. Eis, J. R. Lakowicz, M. L. Johnson, *Eur. Biophys. J.* **1996**, *24*, 185.
[20] M. Ilbert, J. Horst, S. Ahrens, J. Winter, P. C. F. Graf, H. Lilie, U. Jakob, *Nat. Struct. Mol. Biol.* **2007**, *14*, 556.

